ISSN 2176-5480

22nd International Congress of Mechanical Engineering (COBEM 2013)
November 3-7, 2013, Ribeirão Preto, SP, Brazil

INVERSE KINEMATICS FOR GENERAL 6-RUS PARALLEL ROBOTS APPLIED ON UDESC-CEART FLIGHT SIMULATOR

Alexandre Campos
Guilherme de Faveri
Clodoaldo Schutel Furtado Neto
Universidade do Estado de Santa Catarina (UDESC), Centro de Ciências Tecnológicas (CCT), Joinville, Brazil
alexandre.campos@joinville.udesc.br
guilherme.faveri@gmail.com
clo_neto@msn.com

Alexandre Reis
Alejandro Garcia
Universidade do Estado de Santa Catarina (UDESC), Centro de Artes (CEART), Florianópolis, Brazil
a.a.reis@terra.com.br
garcia.ramirez@gmail.com

Abstract. *Abstract. The growth of brazilian aviation industry led to implementation of new manufacturing plants as well as equipment aiming at provide training for pilots. Manufacturing plants will be located in Lages -SC, additionally the Universidade do Estado de Santa Catarina built a flight simulator based on 6-DoF parallel robot which incorporates virtual reality immersion environment. Parallel robots are closed-loop mechanisms presenting very good performances in terms of accuracy, rigidity and ability to manipulate large loads. This paper states a method to compute the inverse kinematics for a generic 6-RUS parallel robot (i.e. 6 serial chains with Rotational, Universal and Spherical joints respectively) based in geometrical constructive aspects. This method manipulates algebraically closed loop equations which led to univocal solution with low computational cost. Additionally, the method is useful tool to compute the flight simulator work space for different orientations.*

Keywords:*Parallel Robot, Flight Simulator, Inverse Kinematic Problem.*

1. INTRODUCTION

Flight simulation has been used in flying industry for many years. Due to the aircraft and pilots training costs, development of many flying training devices became necessary, thus in the decade 1960 use of flight simulator became an integral part of all commercial airline operation and for both safety and training effectiveness, it became no longer practical to train in the actual aircraft (Page, 2010).

Early flight simulators were attempted to achieve the early training effects that was based in graded exercises sequence whIch are realized by the pilot in real aircraft. So the first trainers were ground-based devices able to react to aerodynamic forces, like Sanders Teacher device developed in 1910 (Page, 2010).

Graphic computing progress led flight simulation into virtual reality, but only simulation in virtual environment does not expose pilot to real forces during flight, which cause nausea and discomfort after some hours due to sensorial disconnection between sight and space perception detected by vestibular system, located in inner ear (Carlos S.M. Coelho, 2007).

Other devices used as flight simulators include 3 DoF or 6DoF parallel robots. The spatial parallel robot (6 DoF) are convenient due to full motion possibility. The most used 6 DoF platform is Stewart-Gough platform which is based in 6-UPS (i.e. 6 serial chains with Universal - Prismatic - Spherical joints respectively), that was developed to be used as a full flight simulator. Second most common parallel robot architecture used for flight simulation is 6-RUS, which is approached in this paper.

In Fig. 1 is presented CEART flight simulator and in Fig. 2 the parallel robot structure and the cordinates systems attached to fixed base ${}^{f}O$ and to move platform ${}^{m}O$.

2. PARALLEL ROBOTS

Parallel robots, also named parallel manipulators, typically consist by a moving platform connected to a fixed base by several limbs or legs (Merlet, 2010).

An n-DOF (n-degree-of-freedom) fully-parallel mechanism is composed of n independent legs connecting the mobile platform to the base. Each of these legs is a serial kinematic chain that hosts one or more motors which actuates, directly or indirectly, the chain (Bonev, 2002).

Due to distribution of external load, parallel robots present good performances in terms of accuracy, rigidity and ability

ISSN 2176-5480

Figure 1. CEART flight simulator.

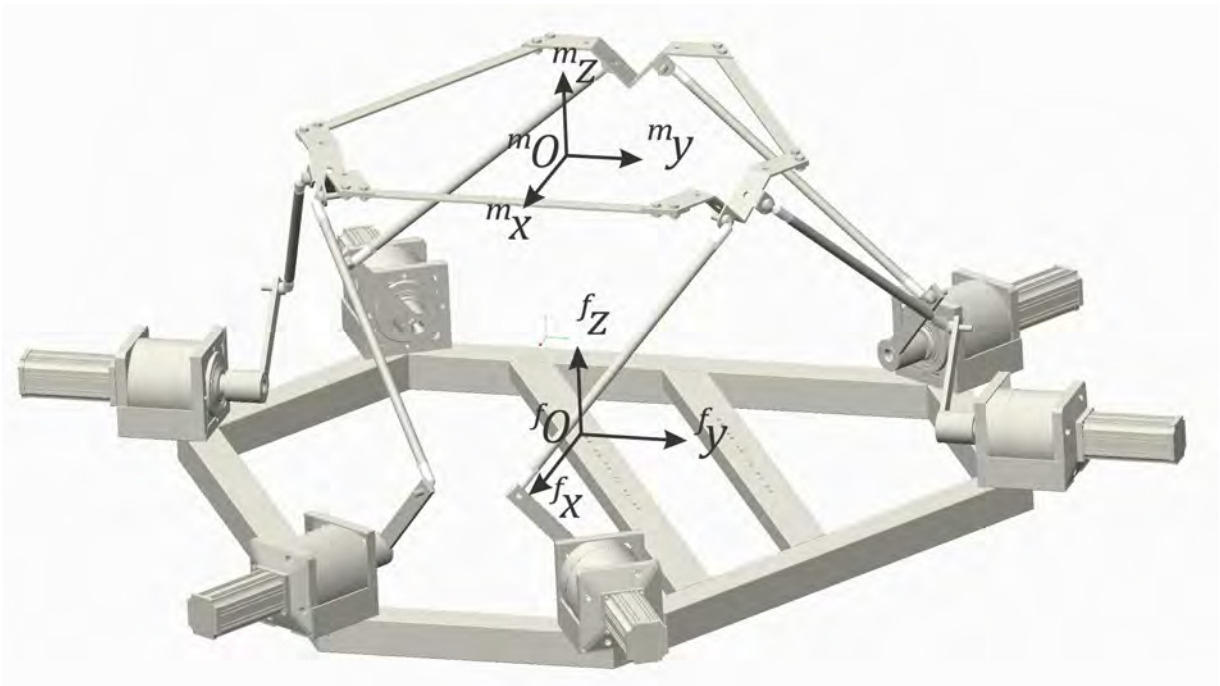

Figure 2. CEART flight simulator robot structure and coordinate systems.

to manipulate large loads (Merlet, 2010).

In the area of 6-DoF parallel robots, the most of researches has been aimed to the 6-UPS architecture known as Stewart-Gough platform as presented in (Advani, 1998), (Fichter, 1986), (Haan, 1995) . The Stewart-Gough platform presents the stiffness architecture due to the only axial load distribution and allows the use of powerful hydraulic actuators. Motion simulators, generally, manipulate excessive loads of up to tens of tons (Bonev, 2002). Besides, the mechanical part, i.e., the robot structure is often only a small fraction of a high-tech flight simulator cost (Bonev, 2002).

The second most common architecture is the 6-RUS kinematic chain, this chain architecture was proposed by Hunt early in 1983 (Merlet, 2010). In this architecture the actuated joint is rotational, which leads to the interchange possibility of universal and spherical joint without any change in mechanism characteristics (Bonev, 2002). As previously mentioned, this paper approaches a method to solve the inverse kinematic problem, which is detailed in next session.

ISSN 2176-5480

3. INVERSE KINEMATIC PROBLEM

For inverse kinematic problem the vector describing moving platform position in cartesian coordinates system and orientation by roll, pitch and yaw angles respectively is given by $P = [P_x \ P_y \ P_z \ \varphi \ \vartheta \ \psi]$.

In this method, few geometrical parameters are necessary to develop the inverse kinematic problem solution for 6-RUS parallel robot. Both of them obtained from a prototype or a CAD model.

Requiered parameters are the fixed base radius r_b, moving platform radius r_p , half-distance between actuated joint pair d, half-distance between joints in moving platform e , crank dimension r_i which is located in active joint, rod dimension Rp , position angle of actuators pair χ_a, position angle of passive spherical joint in moving platform χ_j and the angle between the crank rotational plane and an axis parallel to y β. These parameters are detailed in Fig 3.

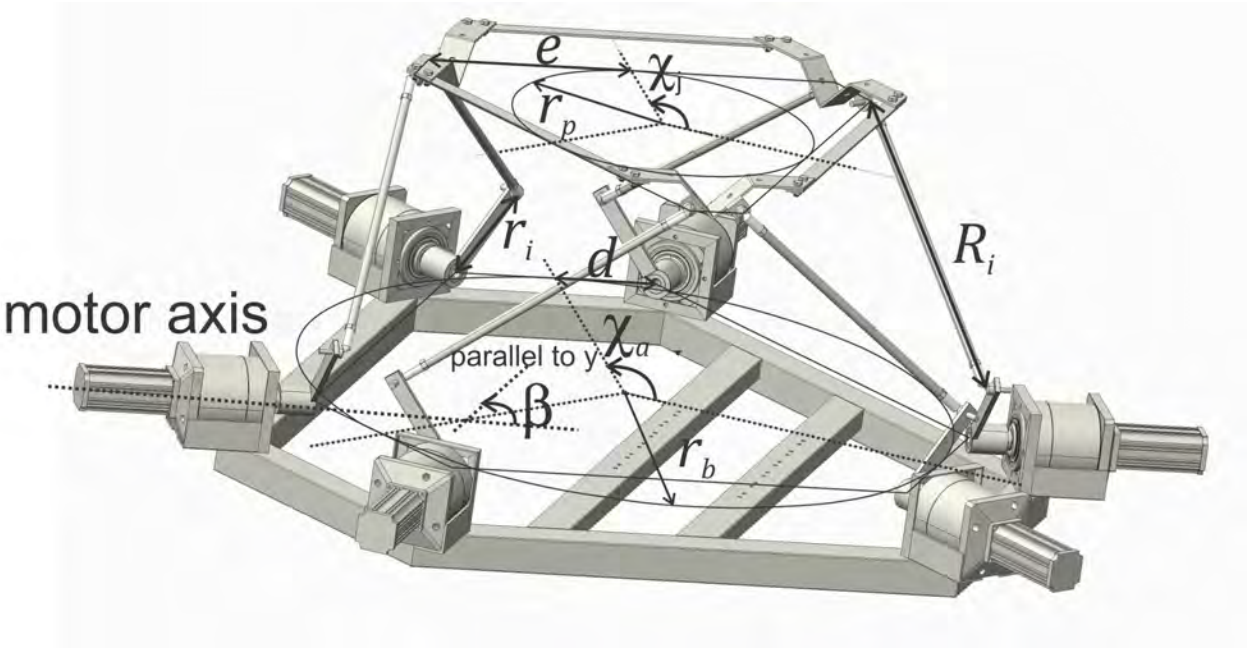

Figure 3. Parallel robot geometrical parameters.

Initially is needed to define the position of the actuators, which can be obtained by Eq. (1) that must be solved for all legs resulting a 6x3 vector:

$$\vec{A} = \vec{R} + \vec{m} \tag{1}$$

$$m = (-1)^{1-i} d \tag{2}$$

Being $i = 1, 2, 3, .., 6$ corresponding to each kinematic chain.

$$\vec{R} = r_b \cos\chi_a \hat{i} + r_b \sin\chi_a \hat{j} \tag{3}$$

$$\vec{m} = -m \sin\chi_a \hat{i} + m \cos\chi_a \hat{j} + 0\hat{k} \tag{4}$$

$$\vec{A} = (r_b \cos\chi_a - m \sin\chi_a)\,\hat{i} + (r_b \sin\chi_a + m \cos\chi_a)\,\hat{j} + 0\hat{k} \tag{5}$$

In same way, all platform joint position, i.e. spherical joint attached to move platform must to be found in local coordinate system attached to moving platform:

$$\vec{C} = \vec{r} + \vec{n} \tag{6}$$

$$n = (-1)^{i-1} e \tag{7}$$

$$\vec{r} = r_p \cos\chi_j \hat{i} + r_p \sin\chi_j \hat{j} + 0\hat{k} \tag{8}$$

$$\vec{n} = -n \sin\chi_j \hat{i} + n \cos\chi_j \hat{j} + 0\hat{k} \tag{9}$$

$${}^m\vec{PC} = r_p \cos\chi_j - m \sin\chi_j \hat{i} + r_p \sin\chi_j + m \cos\chi_j \hat{j} + 0\hat{k} \tag{10}$$

ISSN 2176-5480

The rotational transformation using roll, pitch and yaw angles notation as defined in (Bruno Siciliano, 2009) is used in order to find ${}^{m}\vec{PC}$ from Tool Center Point, attached to move platform origin ${}^{m}O$ to spherical joint in general coordinate system attached to fixed base origin ${}^{f}\vec{O}$.

$$rot = \begin{bmatrix} c\varphi c\theta & c\varphi s\vartheta s\psi - s\varphi c\psi & c\varphi s\vartheta c\psi + s\varphi c\psi \\ s\varphi c\theta & s\varphi s\vartheta s\psi + s\varphi c\psi & s\varphi s\vartheta c\psi - c\varphi s\psi \\ -s\vartheta & c\vartheta s\psi & c\vartheta c\psi \end{bmatrix} \tag{11}$$

$${}^{f}\vec{PC} = rot\ {}^{m}\vec{PC} \tag{12}$$

In order to find vector from actuator to spherical joint $\vec{I}$ the vectorial equation Eq. (13) must be solved.

$${}^{f}\vec{OA} = {}^{f}\vec{OP} + {}^{f}\vec{PC} + {}^{f}\vec{PC} + {}^{f}\vec{I} \tag{13}$$

$$\vec{I} = {}^{f}\vec{OA} - {}^{f}\vec{OP} - {}^{f}\vec{PC} \tag{14}$$

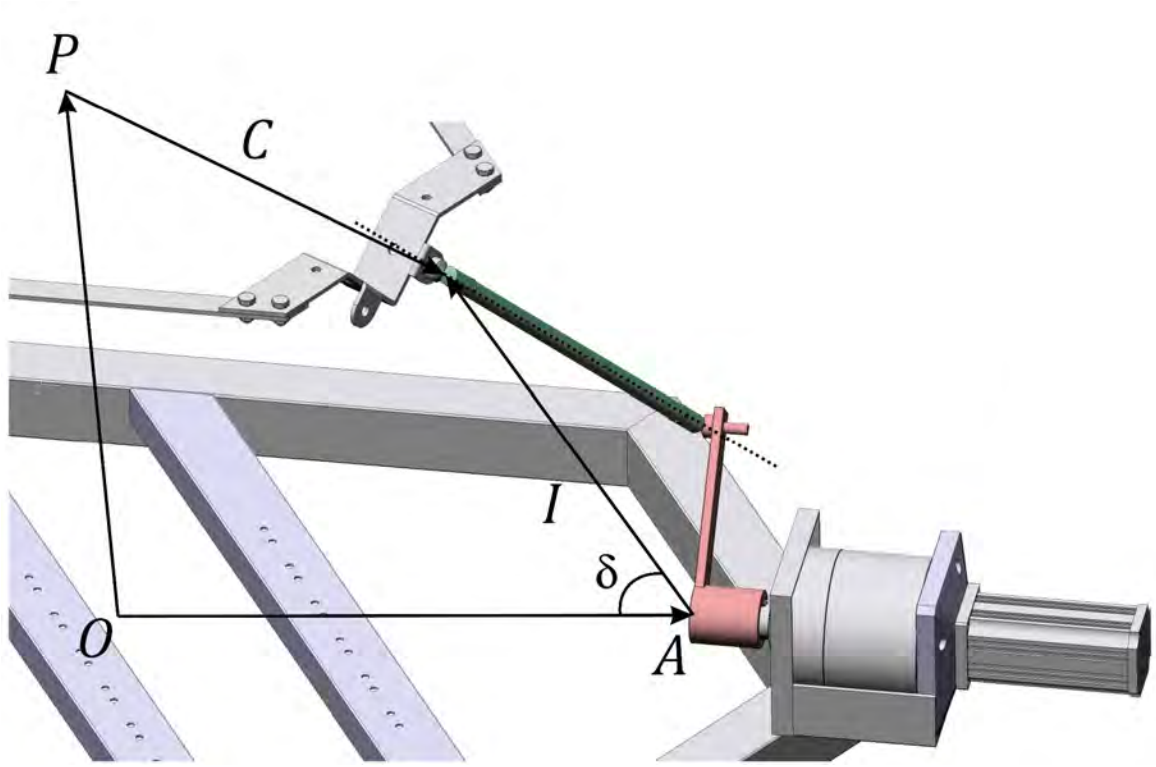

Figure 4. Vectorial chain to i-leg.

The vector $\vec{I}$ may be decomposed in two components, one I_ω in plane ω_i, another one orthogonal to ω_i. The I_ω in ω_i may be decomposed in two components $\vec{I_z}$ and $\vec{T}$, one parallel to the z axis and is contained in plane $_i$ and the other one is parallel to z axis and other one parallel to xy plane, respectively.

$$\vec{I_\omega} = \vec{I_z} + \vec{T} \tag{15}$$

The norm of vector $\vec{T}$ may be written in the components of $\vec{I}$ terms.

$$T = \left\|\vec{T}\right\| = I_x \cos\beta + I_y \sin\beta \tag{16}$$

Where I_x and I_y are $\vec{I}$ components in x and y axis, respectively.

With these definitions, it is possible to analyze crank rotational plane $_i$ and define angles $\theta, \alpha, \phi, \varepsilon$ which must be found to solve inverse kinematic problem, being θ the crank angle.

An analysis in Fig. 5 leads to:

$$\pi = \varepsilon + \phi + \alpha + \theta \tag{17}$$

ISSN 2176-5480

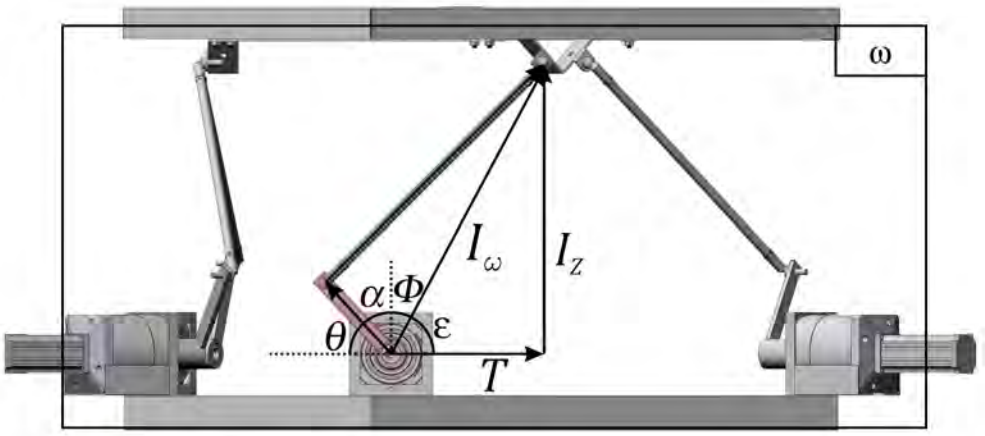

Figure 5. Plane ω_i frontal view and requeried angles

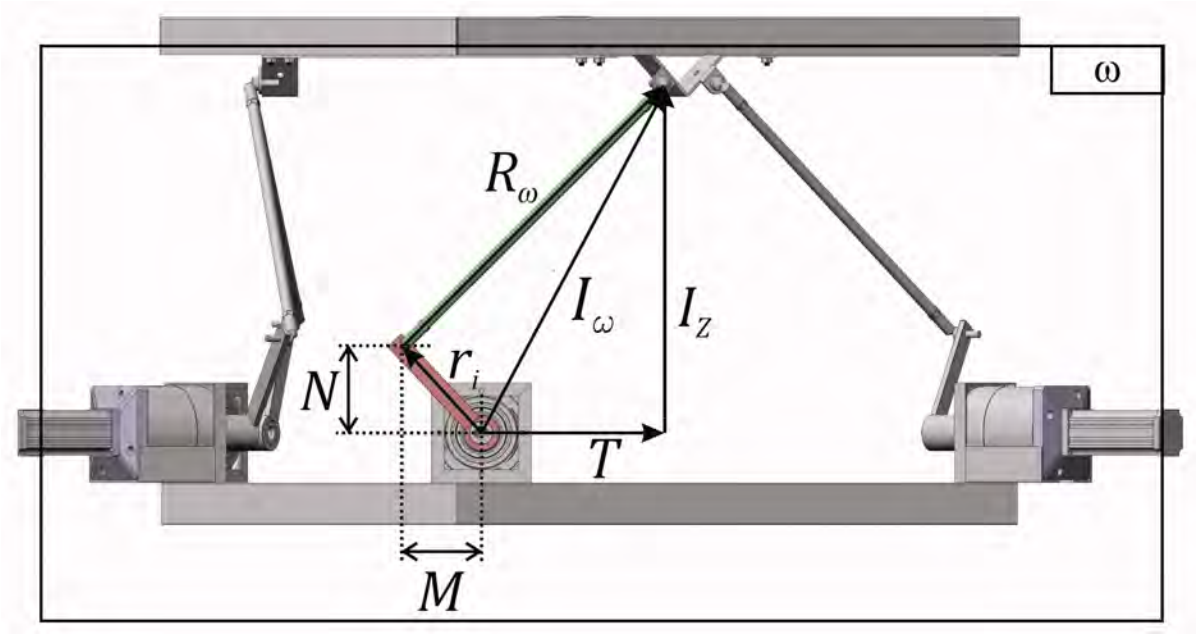

Figure 6. Plane ω_i frontal view.

Using inner product definition and calling M horizontal componente in plane ω_i of $\vec{r}$, and after that multiplying by $2T$ both sides.

$$\vec{r} \cdot -\vec{T} = \|\vec{r}\| \left\|\vec{T}\right\| \cos\theta \tag{18}$$

Where $\frac{-\vec{T}}{\|\vec{T}\|} = -\hat{T}$.

$$-\hat{T} = \hat{r} \tag{19}$$

$$\vec{T} \cdot \hat{r} = M \tag{20}$$

$$M = \|\vec{r}\| \cos\theta \tag{21}$$

$$2TM = 2T \|\vec{r}\| \cos\theta \tag{22}$$

A non-physical parameter u is defined which allows to re-write Eq. (22) as:

$$u = 2Tr_i \tag{23}$$

$$u = \frac{2TM}{\cos\theta} \tag{24}$$

ISSN 2176-5480

Using same method, other non-physical parameter v is defined, however the equation is multiplied by $2I_z$.

$$v = -2I_z \left\|\vec{r}\right\| \tag{25}$$

$$\vec{r} \cdot I_z = \left\|\vec{r}\right\| \left\|\vec{I_z}\right\| \cos\alpha \tag{26}$$

$$N = \left\|\vec{r}\right\| \cos\alpha \tag{27}$$

Where N is vertical component of $\vec{r}$ and the formutaion is similarly to M.

$$2I_z N = 2I_z \left\|\vec{r}\right\| \cos\alpha \tag{28}$$

$$v = \frac{2I_z N}{\cos\alpha} \tag{29}$$

In these terms is it possible to define the relation between $\frac{u}{v}$ and determinate angle ϕ.

$$\phi = \arctan\frac{T}{I_z} \tag{30}$$

$$\frac{u}{v} = \frac{2TM\cos\alpha}{2I_z N\cos\theta} \tag{31}$$

$$\frac{M}{N} = \frac{\cos\theta}{\cos\alpha} \tag{32}$$

$$\frac{u}{v} = -\frac{T}{I_z} \tag{33}$$

$$\phi = -\arctan\frac{u}{v} \tag{34}$$

It is not necessary use this method to find ϕ once I_z and T are known, however since parameters u and v are used after, it is convenient to show the formulation.

An analagous method is applied in order to find other relations to solve the inverse kinematic problem. Calling s the projection of I_ω over $\vec{r}$ and multiplying by $2\left\|\vec{r}\right\|$ for convenience. Also $\left\|\vec{r}\right\|$ is equal to crank lenght, it is substituted by r_i.

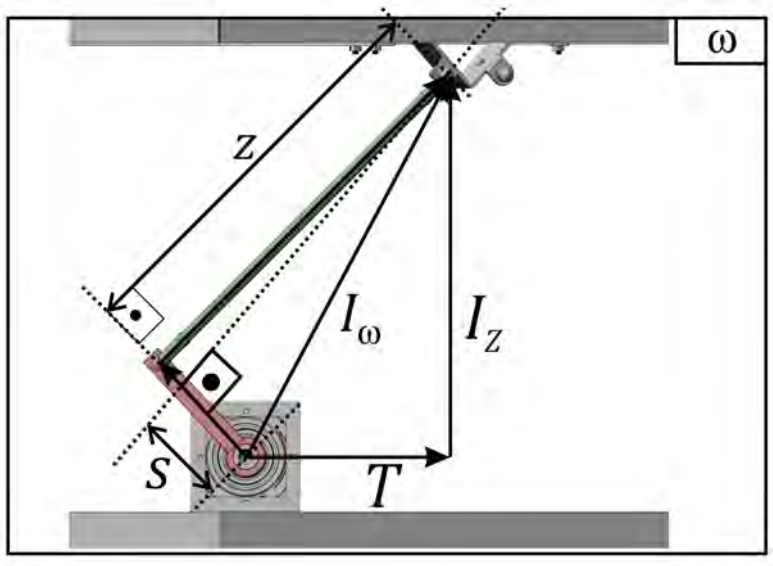

Figure 7. Plane ω_i frontal view.

$$s = \left\|\vec{I_\omega}\right\| \cos(\phi + \alpha) \tag{35}$$

$$2r_i s = 2r_i \left\|\vec{I_\omega}\right\| \cos(\phi + \alpha) \tag{36}$$

ISSN 2176-5480

Using the closed-loop equation it leads:

$$\left\|\vec{R}\right\|^2 = \left\|\vec{I}\right\|^2 + \|\vec{r}\|^2 - \left\|\vec{I}\right\| \|\vec{r}\| \cos\delta \tag{37}$$

Being δ the real angle crank and vector $\vec{I}$. Analysing Eq. (37) in crank rotational plane, it is possible to affirm that $\delta = \alpha + \phi$, and then is defined w, a non-physical parameter.

$$w = -2\|\vec{r}\| \left\|\vec{I_\omega}\right\| \cos\delta \tag{38}$$

$$w = R_i^2 - \left\|\vec{I}\right\| - r_i^2 \tag{39}$$

Also, it is possible to manipulate properly the geometrical equations of triangle rectangle showed in Fig. 7.

$$s^2 = \left(\frac{-w}{2r_i}\right)^2 \tag{40}$$

$$u^2 + v^2 = (2Tr_i)^2 + (-2I_z r_i)^2 \tag{41}$$

$$u^2 + v^2 = (2r_i)^2 (I_\omega)^2 \tag{42}$$

From triangle rectangle showed in Fig. 7

$$z^2 + s^2 = \left\|\vec{I_\omega}\right\|^2 \tag{43}$$

$$(2r_i)^2 z^2 + (2r_i)^2 s^2 = (2r_i)^2 \left\|\vec{I_\omega}\right\|^2 \tag{44}$$

Then is defined other non-physical parameter q and Eq. (44) re-written.

$$q = 2r_i z \tag{45}$$

$$q^2 + (2r_i)^2 s^2 = (2r_i)^2 \left\|\vec{I_\omega}\right\|^2 \tag{46}$$

Substituting Eq. (40) into Eq. (46):

$$q^2 + w^2 = (2r_i)^2 \left\|\vec{I_\omega}\right\|^2 \tag{47}$$

$$q^2 = (2r_i)^2 \left(\left\|\vec{I_\omega}\right\|^2 - \left\|\vec{I_\omega}\right\|^2 \cos(\phi + \alpha)\right) \tag{48}$$

$$q^2 = (2r_i)^2 \left\|\vec{I_\omega}\right\|^2 \sin(\phi + \alpha) \tag{49}$$

$$\frac{q^2}{w^2} = \frac{(2\|\vec{r}\|)^2 \left\|\vec{I_\omega}\right\|^2 \cos^2(\phi + \alpha)}{(2\|\vec{r}\|)^2 \left\|\vec{I_\omega}\right\|^2 \sin^2(\phi + \alpha)} \tag{50}$$

$$\tan(\phi + \alpha) = \frac{q}{w} \tag{51}$$

$$\phi + \alpha = \arctan\frac{q}{w} \tag{52}$$

Returning to Eq. (17).

$$\pi = \varepsilon + \phi + \alpha + \theta \tag{53}$$

$$\varepsilon = \frac{\pi}{2} - \phi \tag{54}$$

$$\pi = \left(\frac{\pi}{2} - \phi\right) + (\phi + \alpha) + \theta \tag{55}$$

$$\theta = \frac{\pi}{2} + \phi - (\phi + \alpha) \tag{56}$$

$$\theta = \frac{\pi}{2} - \arctan\frac{u}{v} - \arctan\frac{q}{w} \tag{57}$$

In these terms, it is solved the inverse kinematic problem. Once function $\arctan$ has a dubious response, it is convenient to use $atan2$ function.

ISSN 2176-5480

4. Results

This paper presented a method to solve the Inverse Kinematic Problem for a 6-RUS parallel robot using some non-physical parameters defined based on the vectorial equation to the chains. Tough the prove of the method is extensive, the application is simple. An algorithm that compute the joint and actuators position and compute the parameter u, v, w and q as presented solve the inverse kinematic problem using really low computational coast.

For convenience Eq. (23), Eq. (25), Eq. (39), Eq. (47) and Eq. (42) may be re-written to compute u, v, w and q based in previously values and apply in Eq. (57).

$$u = 2r_i \left(I_x \cos\beta + I_y \sin\beta\right) \tag{58}$$

$$v = -2r_i I_z \tag{59}$$

$$w = R_i^2 - r_i^2 - I_x^2 - I_y^2 - I_z^2 \tag{60}$$

$$u^2 + v^2 = q^2 + w^2 \tag{61}$$

$$q = \sqrt{u^2 + v^2 - w^2} \tag{62}$$

The same algorithm is useful to find the workspace to a given orientation using some increments to P_x, P_y and P_z and solving the Inverse Kinematic Problem repeatedly it is possible to find the workspace of the parallel robot to a given orientation. The CEART - Flight Simulator workspace is presented in Fig. 8 to a orientation φ, ϑ and ψ equal to zero degrees.

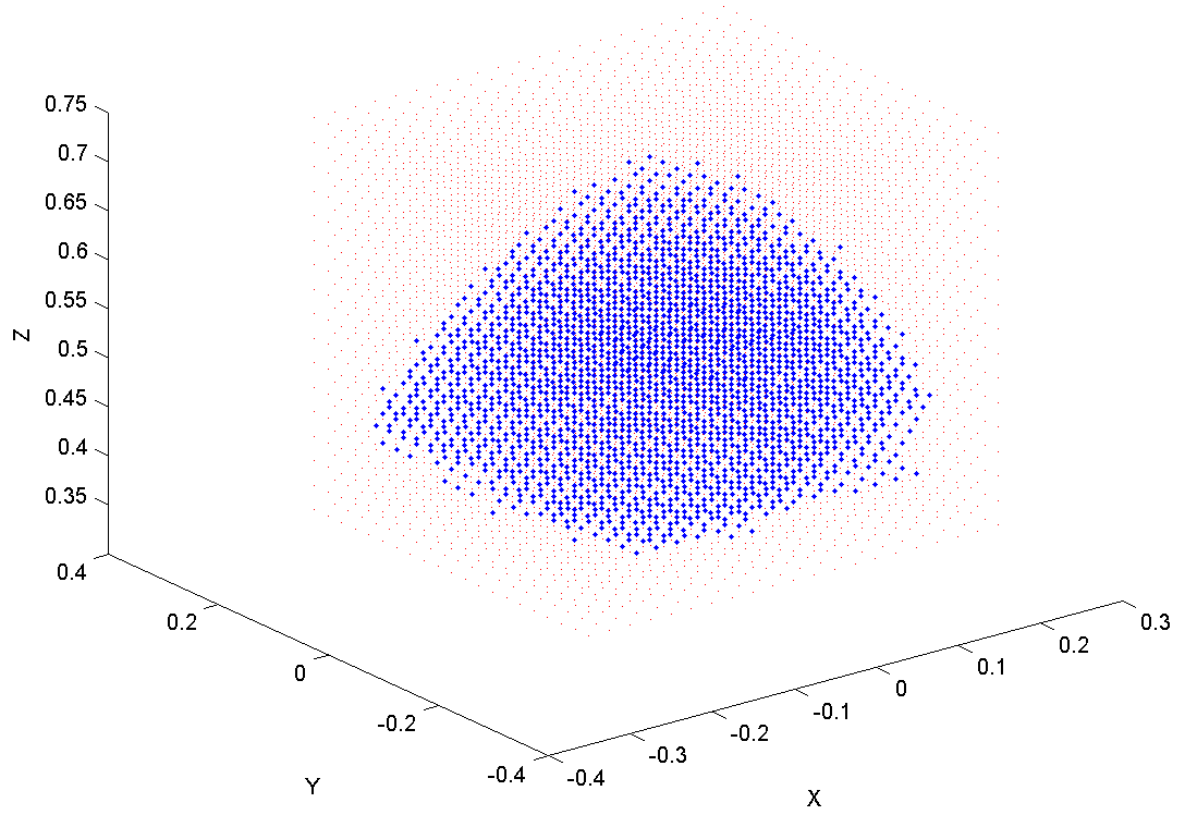

Figure 8. Flight Simulator workspace to $\varphi = 0, \vartheta = 0, \psi = 0$

5. REFERENCES

Advani, S.K., 1998. *The Kinematic Design of Flight Simulatior Motion-Mases*. Master's thesis, University of Toronto.

ISSN 2176-5480

Bonev, I.A., 2002. *Geometric Analysis of Parallel Mechanisms*. Ph.D. thesis, Facult'e des Sciences et de Gt'enie Universalt'e Laval.

Bruno Siciliano, Lorenzo Sciavicco, L.V.G.O., 2009. *Robotics Modeling, Planning and Control*. Springer.

Carlos S.M. Coelho, Jorge A. Santos, C.F.d.S., 2007. "Enjoo de movimento: Etiologia, factores predisponentes e adaptação". In *Psicologia, Saúde & Doenças*.

Fichter, E., 1986. "A stewart based manipulator: General theory and pratical construction". *Internal Journal of Robotics Research*, Vol. 5, pp. 157–182.

Haan, P., 1995. *Design of the Motion System Gimbals of the SIMONA Research Simulator*. Master's thesis, Faculty of Aerospace Engineering, Delft University of Technology.

Merlet, J.P., 2010. *Parallel Robots*. Springer, Dordrecht, The Netherlands, 2nd edition.

Page, R.L., 2010. "Brief history of flight simulation". In *SimTechT 2000 Proceedings*.

6. RESPONSIBILITY NOTICE

The authors are the only responsible for the printed material included in this paper.